



HAL
open science

Coupled effects of simultaneous autogenous self-healing and sustained flexural loading in cementitious materials

Benoit Hilloulin, Carol Youssef-Namnoum, Frédéric Grondin, Ahmed Loukili

► To cite this version:

Benoit Hilloulin, Carol Youssef-Namnoum, Frédéric Grondin, Ahmed Loukili. Coupled effects of simultaneous autogenous self-healing and sustained flexural loading in cementitious materials. *Journal of Building Engineering*, 2023, 79, pp.107895. 10.1016/j.job.2023.107895 . hal-04255477

HAL Id: hal-04255477

<https://nantes-universite.hal.science/hal-04255477>

Submitted on 24 Oct 2023

HAL is a multi-disciplinary open access archive for the deposit and dissemination of scientific research documents, whether they are published or not. The documents may come from teaching and research institutions in France or abroad, or from public or private research centers.

L'archive ouverte pluridisciplinaire **HAL**, est destinée au dépôt et à la diffusion de documents scientifiques de niveau recherche, publiés ou non, émanant des établissements d'enseignement et de recherche français ou étrangers, des laboratoires publics ou privés.

1 **Coupled Effects of Simultaneous Autogenous Self-Healing and** 2 **Sustained Flexural Loading in Cementitious Materials**

3 Benoît Hilloulin*, Carol Youssef Namnoum, Frédéric Grondin, Ahmed Loukili
4 Nantes Université, Ecole Centrale Nantes, CNRS, GeM, UMR 6183, F-44000 Nantes,
5 France

6 * Corresponding author: benoit.hilloulin@ec-nantes.fr; Tel.: + 33 (0) 2 40 37 68 47

8 **Abstract**

9 The self-healing efficiency of cementitious materials might be impaired by external
10 loading. This study investigates the coupled effects of sustained flexural loading and self-
11 healing mechanisms. To this end, prismatic mortar specimens were pre-cracked at two
12 days with 10- μ m wide cracks under bending. Some beams were then immersed for
13 healing and simultaneously loaded for about 4 weeks using an innovative three-point
14 bending test device allowing bending creep displacement measurement. At the same time,
15 reference beams were immersed without load. After the healing period, the specimens
16 were reloaded to assess the effect of creep and healing on the stiffness and strength
17 recovery. It was found that, during immersion, the creep deformation gradually decreased
18 with time, probably due to the precipitation of healing products. However, after
19 immersion, the mechanical properties recovery of specimens undergoing creep during
20 self-healing decreased by 12% compared to the reference specimens. Microscopic
21 observations were consistent with the mechanical recovery measurements, suggesting
22 partial healing of the loaded specimens.

23
24 **Keywords:** self-healing; creep; mortar; early-age; sustained loading; crack.

25 **1. Introduction**

26 Cracking is common in concrete structures, especially at an early age, e.g., during the first
27 days, due to restrained shrinkage, poor relaxation capacity, or slow strength development

28 [1]. For this reason, several expensive concrete structures, such as bridges and marine
29 structures, may inevitably suffer degradation and damage over time due to the ingress of
30 harmful ions, considerably reducing their service life and durability. If the problem is not
31 corrected quickly, cracks become difficult to repair leading to durability, economic and
32 aesthetic issues. Thus, the intrinsic healing ability of concrete could play a valuable role
33 in mechanical and waterproofing aspects to reduce the negative impacts of damage on the
34 durability of concrete structures.

35 Self-healing materials are defined as materials that are capable of partially or fully
36 restoring their impermeability or mechanical properties after healing without human
37 intervention [2]. Self-healing can occur naturally by considering two main mechanisms:
38 a) continuous hydration of residual cement particles with water seeping through cracks;
39 b) calcium carbonate (CaCO_3) formation due to the reaction of CO_3^{2-} dissolved in water
40 and Ca^{2+} ions leaking from the cement matrix into the crack [3,4]. Various studies suggest
41 that the potential of autogenous healing is limited to small cracks and requires the
42 presence of water [5], as opposed to autonomous healing, which is often based on the use
43 of capsules [6–9] or bacteria [10–12] that can become active once the crack appears. In
44 recent years, several studies have been developed to increase the healing potential of
45 cementitious materials and to evaluate the various factors that can influence the amount
46 and precipitation kinetics of healing products. Autogenous healing has been shown to
47 depend on the age of crack formation, the crack width, the presence of mineral additions,
48 or the water-to-cement (w/c) ratio [13–20]. It was found that impermeability can be
49 restored due to calcium carbonate precipitation inside cracks with widths limited to 100–
50 200 μm , regardless of cracking age [21]. However, the healing potential in terms of
51 mechanical recovery is maximized for cracks limited to a few tens of micrometers in
52 width due to the limited extent of the ongoing hydration [22,23]. In addition, continuous

53 immersion into water for several weeks is required to increase mechanical recovery, and
54 regains are generally reported to be limited under cyclic immersion. Furthermore, it is
55 worth noting that stiffness improvements are usually more pronounced than strength
56 recovery, and the latter is only substantial in the case of limited crack width with early
57 age cracking for mortar and concrete [24,25].

58 Preliminary studies have reported that the presence of a sustained compressive load can
59 significantly improve the mechanical recovery of mortar specimens during the healing
60 period by reducing the distance between the crack lips [26]. In some cases, the strength
61 of specimens subjected to 0.5 MPa compressive loading was nearly double that of
62 unloaded specimens. Joseph et al. [27] reported similar results when they observed that
63 the application of compressive stress to 50 μm wide cracks resulted in a beneficial aspect
64 for healing performance. In addition, some studies have reported that constant flexural
65 loading caused unstable mechanical recovery and reduced the self-healing capacity of
66 fiber-reinforced concrete [28–31]. Ozbay and Sahmaran [32] investigated the self-healing
67 behavior of fiber-reinforced Engineered Cementitious Composites (ECC) under different
68 healing environments and showed that constant mechanical loading affected the recovery
69 rate of mechanical properties, such as strength and flexural stiffness. Finally, the
70 detrimental effects of the gradual increase of the sustained creep load on the healing
71 behavior of 180-day-old ECC-type composite cement mixtures under severe conditions
72 have also been reported [33].

73 Therefore, a significant influence of creep on self-healing can be expected based on the
74 previously published work, but it has yet to be quantified for unreinforced cementitious
75 materials. Also, the effect of self-healing on creep deflections under sustained loading has
76 not been addressed. Thus, since such findings could help to explain the behavior of

77 complex structures that are subjected to creep and healing simultaneously, such as
78 bridges, the coupled effects between the two phenomena should be evaluated.
79 This paper presents a new experimental approach using three-point bending creep tests to
80 characterize the behavior of healing cementitious materials subjected to sustained loading
81 at early ages. Mortar specimens were pre-cracked at two days of age using a monotonic
82 three-point bending test to produce a residual 10 μm -wide crack to induce a rapid healing
83 process with noticeable mechanical recovery. The specimens were then immersed in
84 water and subjected to a sustained flexural load for up to 28 days using a dedicated setup
85 to evaluate the effect of creep during healing. The applied sustained load value was set at
86 40% of the ultimate flexural strength of reference mortar specimens. Finally, to clarify
87 the coupled effect of creep and self-healing mechanisms, the recovery of mechanical
88 properties was quantified by reloading the specimens using a three-point bending test and
89 observing the healed cracks under a microscope.

90

91 **2. Experimental program**

92 **2.1 Materials and specimen preparation**

93 Mortar specimens were prepared in a standard mortar mixer with a w/c ratio of 0.4 using
94 CEM I 52.5 Portland cement and 0/4 sea sand (Saremer) with an absorption coefficient
95 of 0.42%. The physical and chemical properties of ordinary Portland cement (OPC) are
96 summarized in Table 1. The mix design of the mortars is reported in Table 2.

97

98 **Table 1.** Mineral compositions and physical properties of cement CEM I 52.5 NF
99 (Villiers au Bouin).

SiO₂	19.6
Al₂O₃	4.5

Chemical composition (%)	Fe₂O₃	2.3
	CaO	63.7
	MgO	3.9
	SO₃	2.6
Physical properties	Specific gravity (kg/m³)	3130
	Specific area (cm²/g)	3900

100

101 **Table 2.** Mortar mix design (kg/m³).

Cement	Sand	Water
709	1231	284

102

103 Unreinforced mortar prisms with dimensions of 40 mm × 80 mm × 300 mm were cast to
 104 assess the creep effect during healing. The selection of the dimensions was made
 105 considering the experimental limitations associated with the feasibility of the immersed
 106 creep test. A 12 mm long stainless steel plate was fixed in the lower center part of the
 107 mold to artificially notch the specimens on one-fifth of their height. The goal was to
 108 initiate one single flexural crack at a specific location using a three-point bending test to
 109 evaluate and compare the self-healing potential of a crack under different healing
 110 conditions.

111 After 1 day of curing under sealed conditions in a room at 20 °C and 85-95% RH, the
 112 specimens were unmolded, and placed in tap water at 20 °C until cracking time at 48 h.

113 All analyses were performed comparing three replicates.

114

115 **2.2 Experimental protocols**

116 **2.2.1 Pre-damage process by three-point bending test and healing conditions**

117 The specimens were pre-cracked at two days of age using a 250 kN press in a three-point
118 bending test controlled by crack mouth opening displacement (CMOD) at a constant
119 opening rate of 0.2 $\mu\text{m/s}$ with a 20 cm span. The load was released when the CMOD
120 equaled 45 μm to obtain a crack tip opening displacement (CTOD) of 10 μm measured
121 using a 2D microscope at 5 locations on top of the notch with $\times 140$ magnification. The
122 choice of an initial crack width of 10 μm created at 48h is representative of thin early age
123 cracks that are likely to enlarge during the first few weeks after cracking. Previous
124 experimental and numerical studies have shown that thin early-age cracks accelerate
125 healing and contribute to better mechanical recovery [25]. Moreover, a limited crack
126 width is easier to handle during creep testing and limits the risk of premature cracking.
127 The specimens were further cured under specific exposure conditions for 26 days up to
128 28 days of age. Two types of aging conditions were studied as described in paragraph
129 2.2.2. Three replicates were fully immersed in tap water at 20 $^{\circ}\text{C}$ with no water
130 replacement to induce self-healing.

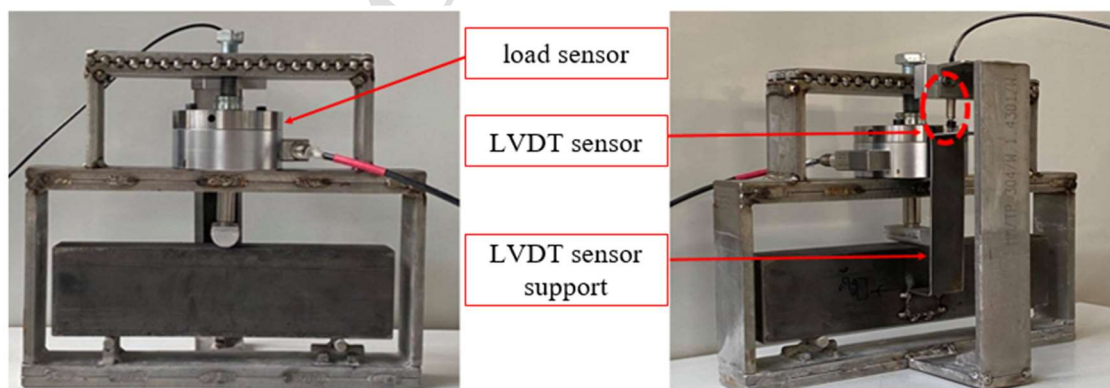
131

132 **2.2.2 Creep measurement during healing**

133 In order to study the effect of self-healing under sustained mechanical loading, a specific
134 three-point sustained flexural loading device was developed. Several reasons supported
135 the development of this new loading device, such as portability and the need to quickly
136 adjust the bending load applied to the low-strength specimens at an early age. In addition,
137 the main advantage of this device lies in the ability to perform early creep tests on pre-
138 cracked beams completely immersed in water to ensure the continuity of hydration of the
139 cement particles. The device was made of stainless steel because it was intended to be

140 used in water and not to generate corrosion products that could affect healing. The
141 thickness of the metal frame was adjusted to limit its deformations while ensuring its
142 portability and both the stability and the limited deformations of the frame were verified
143 using replacement specimens prior to testing.
144 Figure 2 shows the setup for sustained mechanical loading of a prismatic specimen. The
145 specimens were loaded using threaded rods. A load sensor was incorporated into the top
146 part of the frame to evaluate the load applied on the specimens and adjust it in real-time
147 using a dedicated screw. The load was applied at mid-span with a cylindrical tip to ensure
148 a linear load application. Deflection was measured at the center of the beam using an
149 LVDT sensor with a measuring range of ± 0.5 mm and an accuracy of $0.1 \mu\text{m}$, typically
150 used for short-term creep testing [34]. An aluminum stand glued to the center of the beam
151 supported the LVDT sensor and ensured that the sensor was out of the water, as the
152 sensors were not waterproof for long periods of time. Load values were recorded with an
153 accuracy of 5 N.

154



155

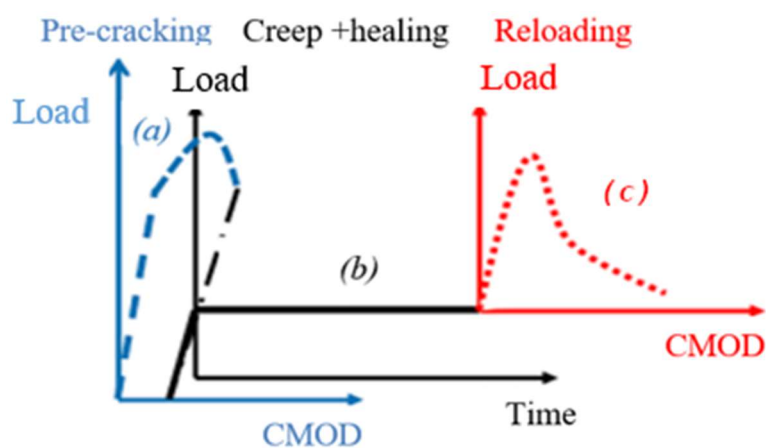
156 **Figure 1.** Three-point flexural loading test setup for measuring creep underwater.

157

158 The specimens were loaded using the following procedure (Fig. 3):

159 a) Initial pre-cracking (see section 2.2.1).

- 160 b) Healing: immersion in water with a constant sustained load for 26 days (40% of
 161 the residual load to avoid nonlinear creep [35]). Reference specimens were
 162 immersed without being loaded.
- 163 c) Reloading: CMOD-controlled three-point bending test to evaluate the mechanical
 164 recovery due to healing by comparing healed and reference specimens (see section
 165 2.2.3).



166 **Figure 2.** Loading principle during the creep-healing test.

168

169 The sustained mechanical loading setup of the prism specimen and the beams was placed
 170 in a tank of water at room temperature of 20 °C (± 2 °C) for 26 days. The water level in
 171 the tank was periodically adjusted over time to prevent the beams from drying out during
 172 the tests.

173 The load level remained constant throughout the tests at 40% of the ultimate flexural load
 174 of the beam. Table 3 summarizes the ultimate flexural strength for the cracked specimens
 175 and the constant sustained load applied to the two types of loaded specimens. The values
 176 of the applied load during the creep tests were derived by taking 40% of the maximum
 177 bending load at the age of cracking. Manual load adjustment was performed by turning
 178 the load screw after 1 hour and twice during the first 24 hours to ensure constant load. At

179 the same time, cracked specimens without continuous mechanical loading and uncracked
180 specimens were kept in the same water tank as references.

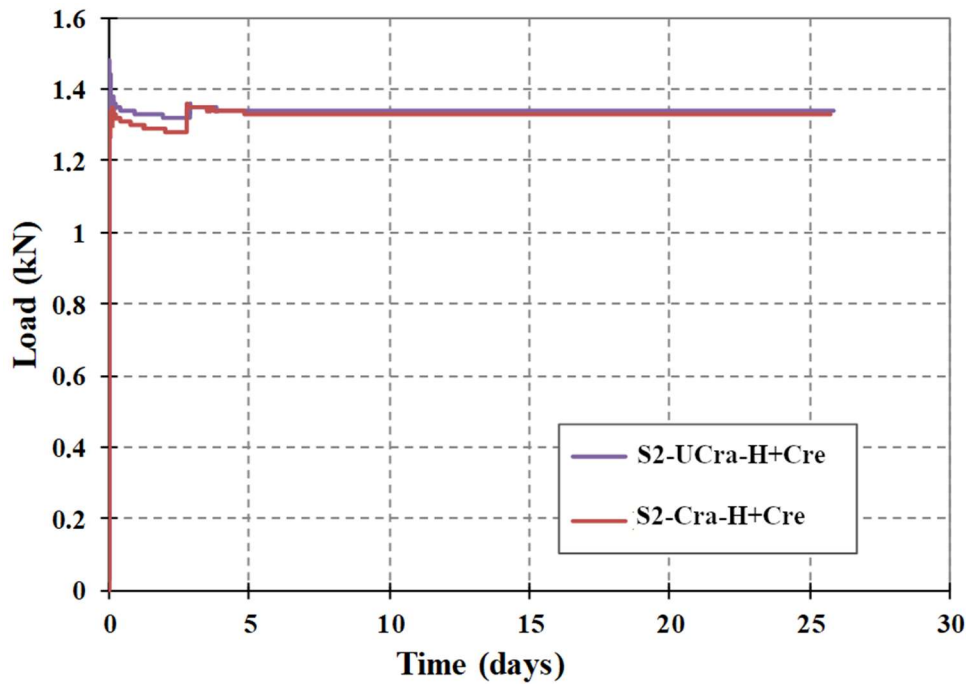
181 For the uncracked beams, the value of the constant load for the creep test was the same
182 as for the healed beam prepared during the same casting. Fig. 4 shows the evolution of
183 the applied load for the two types of beams (S2-UCra-H+Cre and S2-Cra-H+Cre the
184 uncracked beam, and the cracked beam, resp., subjected to creep during immersion). As
185 shown in the figure, only a relatively limited relaxation occurred during the first five days.
186 The applied load was manually increased for about three days to limit the relaxation. The
187 complete program is shown in Fig. 5.

188

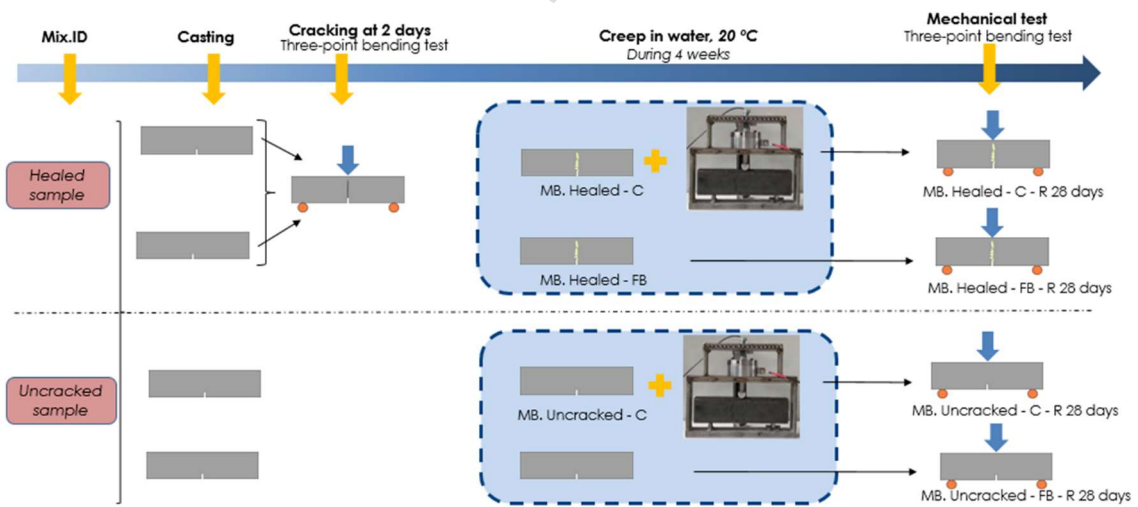
189 **Table 3.** Flexural strength and creep load applied to mortar specimens subjected to creep
190 during healing.

Tested specimens	Flexural load – 2 days (kN)	Constant load for 26 days (kN)
S2-Cra-H+Cre	3.47	1.3
S2-UCra-H+Cre	-	1.3

191



192 **Figure 3.** Load applied to the mortar specimens tested during the coupled test creep-
 193 self-healing.
 194
 195



196 **Figure 4.** Creep – healing test program of mortar beams (MB refers to the mortar beam,
 197 C the creep loading and FB free bending).
 198

199 **2.2.3 Reloading and quantification of mechanical recovery healing**

200 The final step of the experimental program was to reload the pre-damaged and uncracked
 201 specimens under three-point bending to characterize their residual mechanical behavior.
 202

203 For this purpose, the specimens were removed from water and three-point bending tests
204 were performed after a drying period of 1 h at 20 °C and ambient relative humidity to
205 limit the effect of humidity on the measurement of mechanical recovery, as explained in
206 [19].

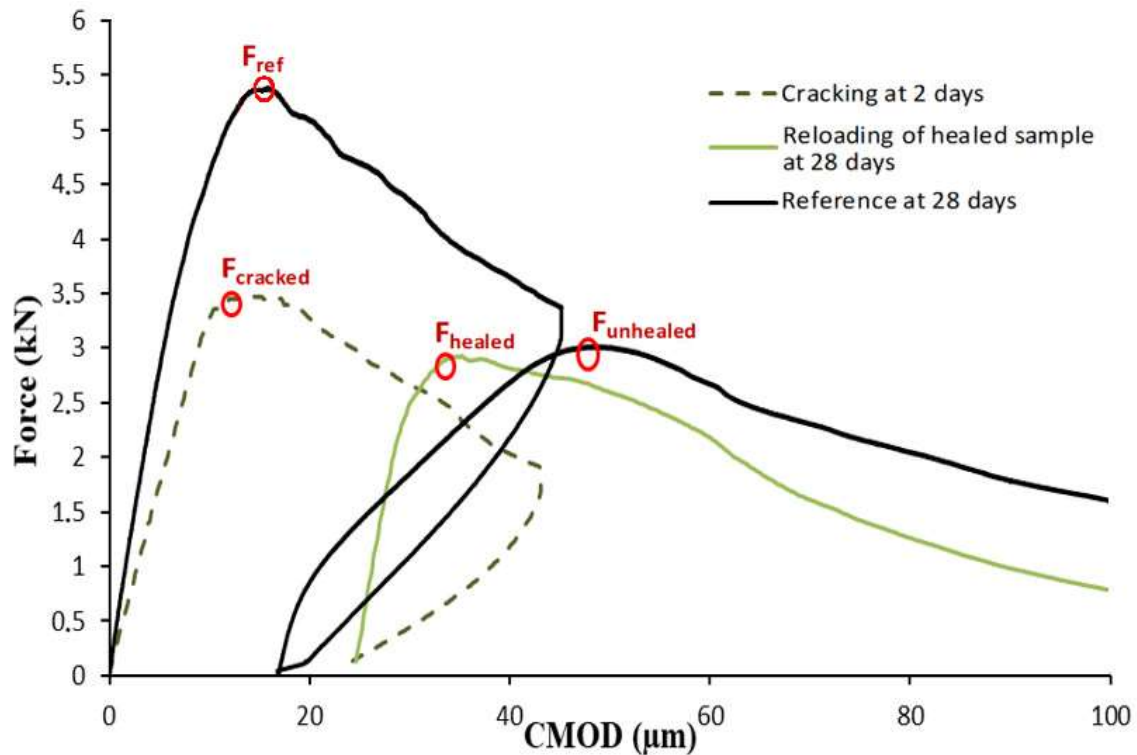
207 In this step, the flexural load-deflection curve obtained when the cracked specimens were
208 mechanically reloaded was compared with the load curves of the reference specimen that
209 had undergone the same curing conditions [36].

210 Healing efficiency was quantified by using two mechanical recovery ratios related to
211 strength recovery [37]:

$$R_1 = \frac{F_{cracked}}{F_{ref}} \quad (1)$$

$$R_2 = \frac{F_{healed}}{F_{unhealed}} \quad (2)$$

212 Where $F_{cracked}$ represents the maximum strength of the specimen during cracking at 2
213 days, F_{healed} the maximum strength of the healed specimens during reloading, F_{ref} the
214 maximum strength of the reference specimen loaded at 28 days, $F_{unhealed}$ the maximum
215 strength of the reference specimen during reloading, as represented in Fig. 6. Mean values
216 and standard deviations of the ratios were calculated and reported to evaluate the effect
217 of creep during self-healing on the final mechanical recovery.



218

219 **Figure 5.** Example of load vs. CMOD curves for specimens submitted to creep healing
 220 and reference specimens; representation of quantities for calculation of mechanical
 221 indexes.

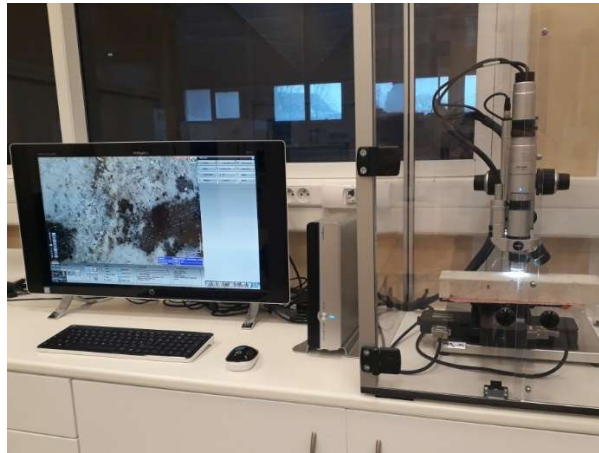
222

223 **2.2.4 Microscopic observations**

224 Microscopic images of the cracks were taken using a Hirox RH 3000 3D optical
 225 microscope at $\times 50$ to $\times 400$ magnification. Under the microscope, several tracking marks
 226 were manually drawn on the specimens after cracking using a fine blue pen, and the
 227 corresponding images were saved as references. After the healing period, images of the
 228 same locations were taken to monitor the evolution of the crack width just before the
 229 beam was reloaded, as described in 2.2.3. Special care was taken in handling the
 230 specimens to avoid accidental breakage after creep. In addition, a thin sheet of paper was
 231 placed between the specimen and the metal motorized stage to prevent scratching of
 232 healing components, as illustrated in Fig. 6.

233

a)



b)



234 **Figure 6.** Photograph of the specimen observation under the optical microscope: a)
235 global view, b) close-up view of a specimen placed horizontally on top of a paper sheet.

236

237 **2.2.6 Summary of the experimental program**

238 Table 4 summarizes the specimens tested and the different healing, creep, and three-point
239 reloading conditions. Three specimens were healed and subjected to creep or not to
240 evaluate the coupled effect between healing and creep, and additional references
241 (uncracked or unhealed) were prepared to compare the behavior with results already
242 published in the literature. The designation of the specimens works as follows: ‘Cra’ or
243 ‘Ucra’ is written depending on whether the specimen was cracked at two days or not, ‘H’

244 or ‘NoH’ is given if the specimen was immersed for healing or not, and ‘Cre’ or ‘NoCre’
 245 ends the denomination depending on whether the specimen was subjected to creep.
 246 Hyphens ‘-’ are used to separate two successive steps while plus signs (‘+’) are used for
 247 simultaneous actions, e.g., simultaneous healing and creep is written as ‘H+Cre’.

248

249 **Table 4.** Summary of the specimens and cracking, healing, and creep conditions.

	Nb specimens	Initial Cracking	Healing + creep	Healing without creep	Reloading
S2-Cra-H+Cre	3	✓	✓		✓
S2-Cra-H+NoCre	3	✓		✓	✓
S2-UCra-H+Cre	3		✓		

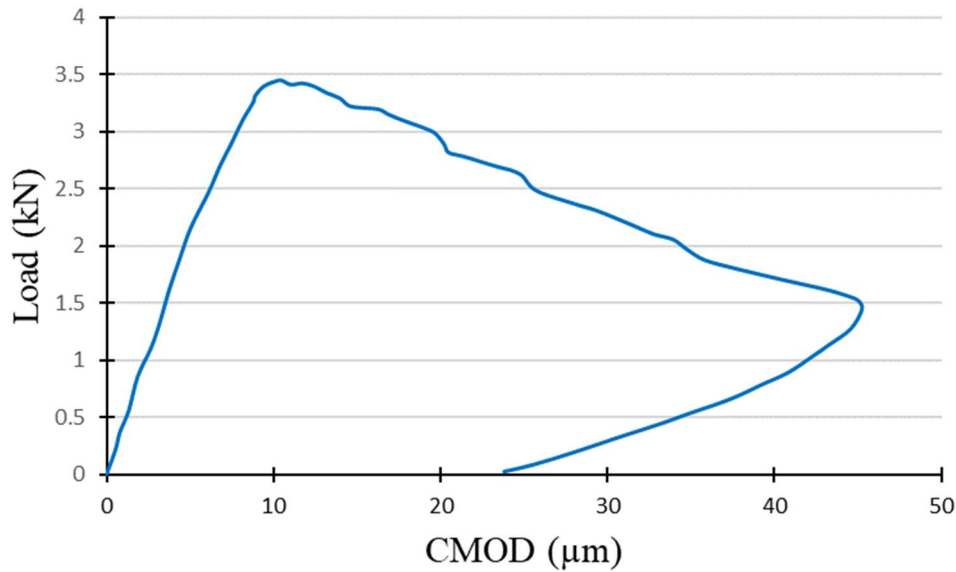
250

251 3. Results and discussion

252 3.1 Failure properties during the pre-cracking stage

253 Fig. 7 shows typical load curves as a function of the CMOD measured during the pre-
 254 cracking phase at 2 days. The maximum strength of the specimen was 3.4 kN. The peak
 255 load occurred at CMOD values of 25 μm . After the peak load, the crack width increased
 256 and the load was removed when the CMOD reached 45 μm in order to obtain an actual
 257 crack width close to 10 μm as observed with a microscope (corresponding to a mean final
 258 CMOD after unloading of 23.8 μm). The variability of the ultimate strength and final
 259 crack characteristics was evaluated by analyzing the load curves and microscopic image
 260 analysis, as shown in Table 5. Such a limited final crack width has been previously
 261 reported to influence healing positively [25,38], and the reduced crack width variability
 262 ensures the best possible repeatability during the healing phase.

263



264
265 **Figure 7.** Evolution of typical load vs. CMOD curves during cracking by three-point
266 bending, at 2 days.

267
268 **Table 5.** Maximum strength and crack characteristics with standard deviations after the
269 pre-cracking stage.

Maximum Flexural load (kN)	Final CMOD value (μm)	Measured crack width (μm)
3.47 ± 0.15	23.8 ± 1.4	9.9 ± 0.4

270

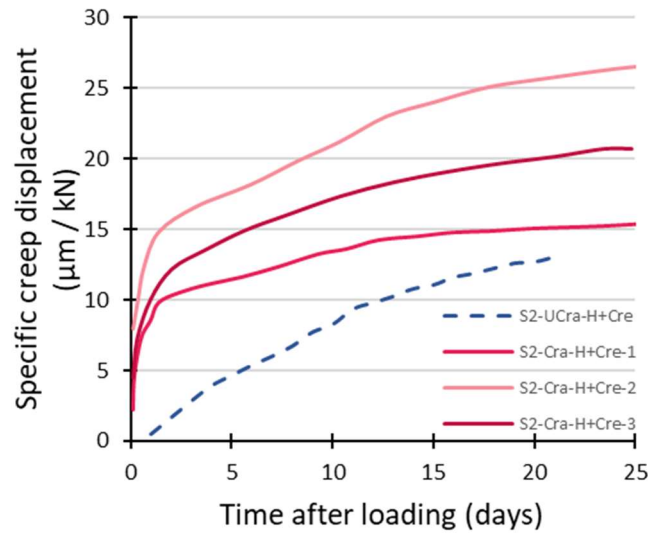
271 3.2 Creep behavior of cementitious materials during self-healing

272 Figure 8 shows the specific creep displacement of specimens loaded in water during
273 healing. During the coupled creep-healing test, a rapid progression of creep displacement
274 was observed during the first day after loading during the coupled creep-healing test. In
275 fact, the value of the specific creep displacement of the precracked specimens ranged
276 from 10 to 15 $\mu\text{m} / \text{kN}$, which was about four times the value of the creep displacement
277 of the uncracked specimens subjected to the same sustained mechanical load

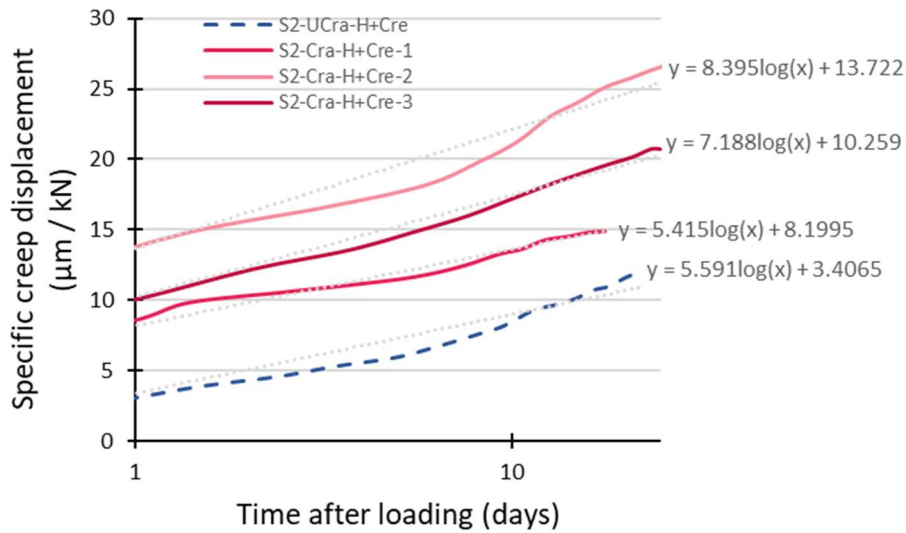
278 (3.5 $\mu\text{m} / \text{kN}$). This can be explained by the absence of healing products immediately
279 after cracking and a low precipitation rate for a short healing period of only one day.
280 After one day of healing, when the specimens were 3 days old, the creep displacement
281 slowed down with time for all the healing specimens, especially for specimens 1 and 2.
282 The slowing of the creep displacement in the healing specimens indicates that progressive
283 self-healing limits the progression of creep displacements. Between 1 day and 24 days of
284 healing under creep, the specific creep displacement increased by 5.4, 11.5 and
285 10.6 $\mu\text{m} / \text{kN}$ for specimens 1, 2 and 3, resp., while the specific creep displacements
286 progressed by 8.7 $\mu\text{m} / \text{kN}$ in the mean uncracked reference specimen. Therefore, the
287 specific creep displacement during this period was smaller for one specimen subjected to
288 creep and healing than for the reference, indicating a rapid progression of healing under
289 creep, while the other healing specimens exhibited a relatively rapid increase in specific
290 creep displacement. This is similar to what was reported in [32], where crack self-healing
291 in fiber-reinforced engineered concrete was measured under creep loading. This
292 observation is also consistent with the fact that a load that closes or limits the crack width
293 can help achieve better healing [39].
294 As can be seen in Fig. 8 b), the progression of creep in the healing specimens followed
295 relatively well a logarithmic behavior, although the specific creep displacement was
296 particularly slow in specimens 1 and 2 between days 1 and 10 before a relative increase
297 in speed. This could be related to the precipitation of new healing products in the crack,
298 with a stiffness close to that of the primary products of normal hydration mechanically
299 binding the crack faces.
300 Bazant and Prasannan [40] linked this short-term aging in amplitude and kinetics to the
301 evolution of the hydration process. The increase in the volume fraction of the hydrates
302 induces an increase in the structural stiffness. This affects the amplitude of creep

303 deformations, which decreases with aging. The increase in the volume fraction of
304 hydrates also influences the viscoelasticity of the material and then the creep kinetics.
305 Therefore, the continuous hydration of cement particles appears to limit the propagation
306 of creep displacement due to self-healing. The particularly important slowing of creep in
307 healed specimens n°2 and 3 could also be attributed to the precipitation of healing
308 products, which are less prone to creep than in the reference matrix. This behavior could
309 be attributed to the precipitation of more calcium carbonate-based products, which were
310 found to be one of the main healing products.

a)



b)



311 **Figure 8.** Specific creep displacement of the healed beams loaded with constant sustained
 312 load (specimens 1 to 3) and the reference mean uncracked beam loaded with constant
 313 sustained load: a) linear time scale, b) logarithmic time scale with regressions.

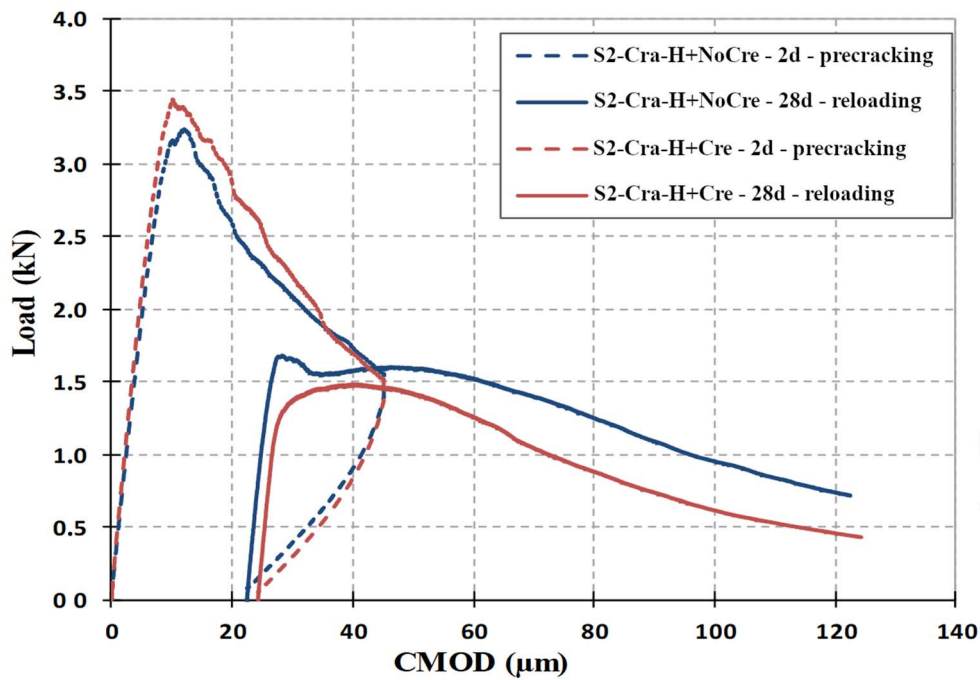
314

315 Healing variability, which has been demonstrated both in the case of mechanical [7, 12,
 316 13, 24] and impermeability recovery [3, 6, 7, 14] after healing, can also be evidenced in
 317 the case of creep properties during healing. As previously explained, one out of the three
 318 specimens that healed while undergoing creep exhibited a decreasing creep rate over the
 319 study period, resulting in specific creep displacements between the first and the twentieth
 320 day after loading that were smaller than the uncracked reference specimens, while the
 321 other two specimens exhibited a decreasing creep rate but still deflected more than the
 322 uncracked reference specimens after 20 days. Although this difference between the three
 323 behaviors can be considered relatively limited, it can be hypothesized that the creep
 324 displacements of the healing specimens may diverge slightly over time; the better the
 325 healing, the slower the creep.

326

327 **3.3 Recovery of mechanical properties by self-healing during creep**

328 Fig. 9 shows typical flexural load-CMOD curves obtained for beam specimens prepared
329 with the same mortar mix and subjected to the two different exposure regimes, i.e., with
330 or without continuous loading. In this figure, it can be seen that each curve has two parts:
331 the pre-cracking phase, consisting of loading and unloading, and the reloading phase,
332 immediately or after healing. It can be observed that there is a loss in residual flexural
333 strength of about 12% for the specimens healed under creep compared to the specimens
334 healed in water without sustained load (1.45 kN and 1.65 kN resp.). For both specimens,
335 a quasi-bilinear behavior is observed during the pre-peak phase, with the recovery of the
336 original stiffness of uncracked specimens. In addition, for the specimen healed without
337 load (S2-Cra-H+NoCre), a sharp drop is observed after the initial stiffness recovery. It is
338 likely that the crack propagates progressively in the specimens that have undergone creep,
339 compared to the other healed specimens where the cracks propagate more rapidly. This
340 sharp peak observed for the healed beams during reloading (S2-Cra-H+NoCre) can be
341 explained by the fact that the cracks are partially filled with new crystals that form during
342 healing, and therefore the initiation of the damage is different in the healed and unhealed
343 areas, as observed in [41]. These localized healing products are unable to withstand the
344 increasing load and crack initiation, which quickly triggers the brittle behavior of the
345 structure.

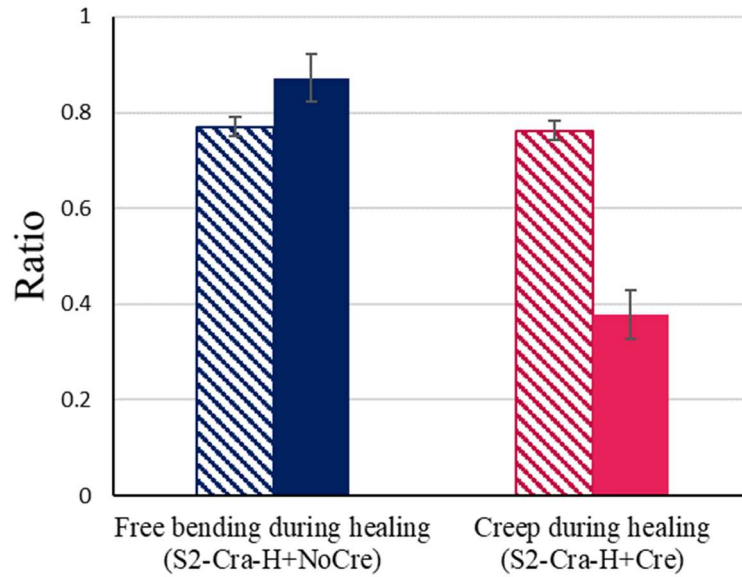


346

347 **Figure 9.** Comparison of load - CMOD curves for creep - healed beams and healed
 348 beams after a 26-day water immersion period.

349

350 To illustrate the effects of sustained mechanical loading on the recovery of mechanical
 351 properties after the healing process, Fig. 10 shows the above-defined ratios for all the
 352 specimens tested. As shown by the R_2 ratio, the strength recovery of the pre-cracked
 353 specimens exposed to water under sustained mechanical loading decreased compared to
 354 the specimens exposed to the same environment but not subjected to sustained mechanical
 355 loading. Once reloaded after self-healing, a reduction in the flexural strength ratio from
 356 0.87 to 0.38 can be observed for specimens subjected to mechanical load during water
 357 exposure. In the case of specimens without mechanical loading, the experimental results
 358 show a slightly increased flexural strength value after the healing mechanism.



359

360

Figure 10. Influence of creep loading on mechanical regains defined by R₁ and R₂

361

indices and associated standard deviations (R₁: hatched, R₂: plain).

362

363

The decrease in mechanical properties of specimens stored in water with sustained

364

mechanical loading can be attributed to the reopening of microcracks created during the

365

pre-cracking phase at a young age. According to Rossi et al. [42], continuous loading at

366

an early age leads to the propagation of internal microcracks created at the time of

367

loading. The propagation of narrow cracks occurs around many anhydrous cement

368

particles. Thus, they represent water access paths that allow the ongoing hydration of

369

anhydrous clinker particles (self-healing). Therefore, the lower self-healing performance

370

of the pre-cracked specimens cured in water is due to the prolonged mechanical loading

371

applied to the pre-cracked specimens.

372

The mechanical properties recovery of specimens exposed to creep during healing were

373

found to be lower than the properties of specimens that were healed without undergoing

374

creep. This can be attributed to the increase in the distance between the two crack faces

375

during healing due to creep, which probably creates a more porous structure of the healing

376

products, having an opposite effect to the densification produced locally by creep.

377 Thus, the present experimental study has made it possible to clarify the coupled effect
378 between creep and self-healing behavior. It was observed that self-healing reduces the
379 progression of creep displacements. This result is probably due to the reconstitution of
380 the connection between the crack surfaces by the self-healing mechanism. However,
381 when a sustained load was applied to the pre-cracked specimens during the healing
382 period, the level of mechanical property recovery as a result of self-healing was reduced.

383

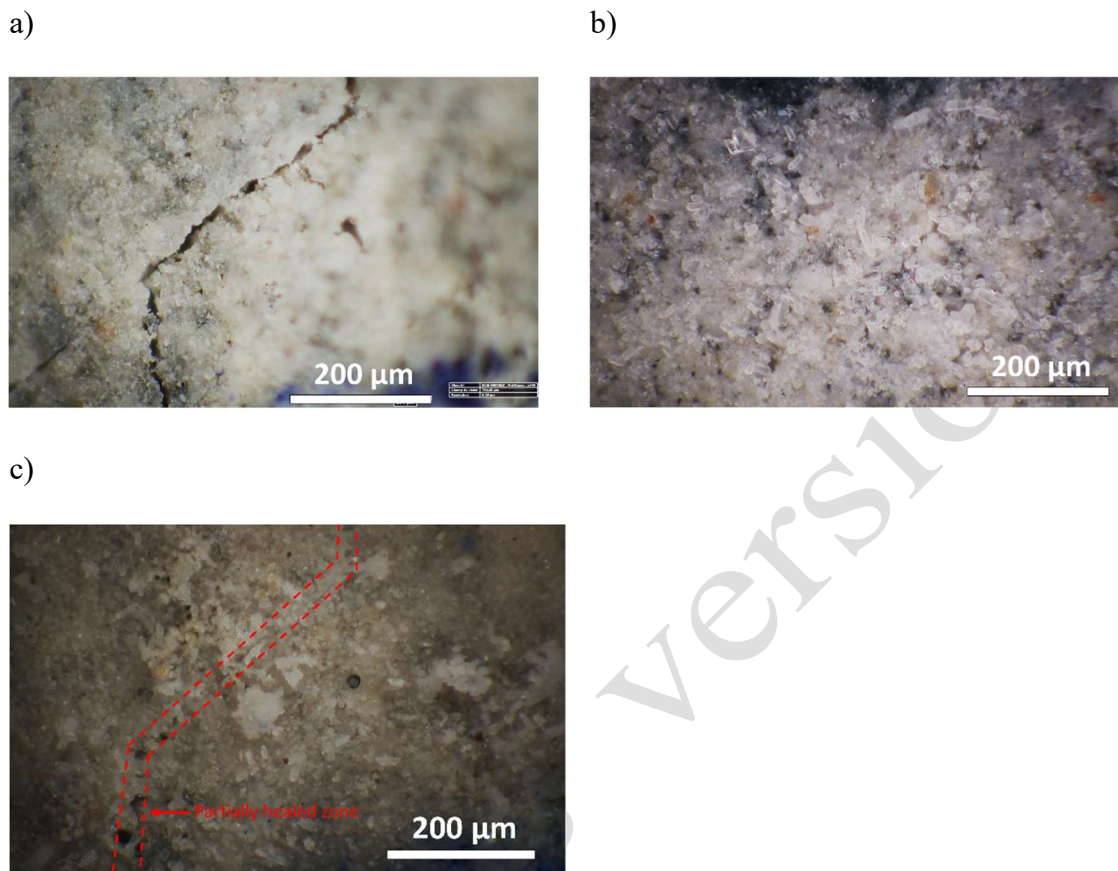
384 **3.4 Microscopic observations**

385 Microscopic observations support the abovementioned mechanical findings. As
386 illustrated in Fig. 11, all the cracks showed very good overall healing due to the early-age
387 crack initiation. Fig. 11 a) is an image of the largest portion of the bottom part of an initial
388 crack prior to healing. In this image, the initial crack width was approximately 9 μm to
389 17 μm . Since the specimen is made of mortar, the crack does not show branching but its
390 orientation varies locally depending on the presence of sand particles. Similar initial crack
391 widths close to the one reported in Table 5 were observed on the other specimens.

392 After the healing period, white products were observed almost all along the cracks
393 initially present on the S2-Cra-H+NoCre specimens, as illustrated in Fig. 11 b). The initial
394 crack path shown in the image is barely visible. This finding agrees with the previously
395 published studies on the very good autogenous healing capacity of thin early-age cracks
396 [43]. These white products visible at the surface are mostly calcium carbonate
397 polymorphs, and locally cloudy-like CSH was observed [25].

398 Conversely, it has been observed that healing products did not cover the entire crack
399 surface of the specimen subjected to sustained loading (S2-Cra-H+Cre). As illustrated in
400 Fig. 11 c), some zones of the initial crack were not filled with healing products, such as
401 the lower left part of the crack in the given image. This observation is consistent with the

402 lower mechanical recovery observed for mortar specimens, which can be attributed to the
403 lower healing capacity of mortar specimens subjected to creep, as suggested by [44].



404 **Figure 11.** Microscopic images of the bottom parts of the cracks of two typical
405 specimens: a) after cracking, b) after healing without loading, and c) after simultaneous
406 healing and creep (initial crack path is given in dashed line).

407

408 **4. Conclusions and perspectives**

409 The objective of this paper was to experimentally determine the coupled effect of
410 sustained mechanical loading and autogenous self-healing mechanisms on the mechanical
411 behavior of mortar specimens pre-cracked at an early age (2 days) and healed for three
412 weeks. To this end, a series of mortar specimens were simultaneously loaded and healed
413 for three weeks using an innovative and specific setup. Based on the results, the following
414 main conclusions can be drawn:

- 415 • Creep deformation was reduced during self-healing due to the gradual
416 precipitation of healing products in the cracks, and healing specimens subjected
417 to creep exhibited an intermediate behavior between cracked and uncracked
418 specimens.
- 419 • The specific creep displacements were significantly higher in the cracked
420 specimens than in uncracked reference specimens, but after one day of healing,
421 the displacement rate slightly decreased with time and became smaller for one out
422 of the three tested specimens, and finally followed a logarithmic trend.
- 423 • The slow improvement in strength recovery due to self-healing was reduced by
424 12% for specimens subjected to continuous mechanical loading during healing,
425 and specimens subjected to creep during healing had lower strength than healed
426 specimens that were not subjected to creep. The application of a constant load is
427 likely to increase the crack width in the mortar beams, which may negatively
428 affect the self-healing process.
- 429 • Microscopic observations confirmed the very good healing capacity of the
430 specimen, which explains the mechanical recovery. However, the self-healing
431 phenomenon seems to be influenced by creep.

432 These results open up new avenues of research on the self-healing capacity of
433 cementitious materials subjected to prolonged loading, particularly with regard to the
434 ultimate recovery potential and the development of healing at an early age. In the future,
435 it would be interesting to study a constant loading level in order to consider the evolution
436 of the properties of the healing material in water and, finally, to define a loading threshold
437 above which self-healing remains predominant over creep.

438

439 **Acknowledgments**

440 The authors would like to thank Vincent Wisniewski and Mathias Marcel (GeM, Ecole
441 Centrale de Nantes) for their assistance during the experiments.

442
443 **References**

- 444 [1] J. Kheir, A. Klausen, T.A. Hammer, L. De Meyst, B. Hilloulin, K. Van
445 Tittelboom, A. Loukili, N. De Belie, Early age autogenous shrinkage cracking risk
446 of an ultra-high performance concrete (UHPC) wall: Modelling and experimental
447 results, *Engineering Fracture Mechanics*. 257 (2021) 108024.
448 <https://doi.org/10.1016/j.engfracmech.2021.108024>.
- 449 [2] C. Edvardsen, Water Permeability and Autogenous Healing of Cracks in Concrete,
450 *ACI Materials Journal*. 96 (1999) 448–454.
- 451 [3] C. Edvardsen, Water permeability and autogeneous healing of cracks in concrete,
452 *ACI Materials Journal*. 96 (1999) 448–454. <https://doi.org/10.14359/645>.
- 453 [4] N. Hearn, Self-sealing, autogenous healing and continued hydration: What is the
454 difference?, *Materials and Structures/Materiaux et Constructions*. 31 (1998) 563–
455 567. <https://doi.org/10.1007/bf02481539>.
- 456 [5] K. Van Tittelboom, N. De Belie, E. Schlangen, Self-Healing Phenomena in
457 Cement-Based Materials Self-Healing Phenomena in Cement-Based Materials,
458 2013.
- 459 [6] C. Dry, Matrix cracking repair and filling using active and passive modes for smart
460 timed release of chemicals from fibers into cement matrices, *Smart Materials &
461 Structures*. 3 (1994) 118–123.
- 462 [7] B. Hilloulin, K. Van Tittelboom, E. Gruyaert, N. De Belie, A. Loukili, Design of
463 polymeric capsules for self-healing concrete, *Cement and Concrete Composites*.
464 55 (2015) 298–307. <https://doi.org/10.1016/j.cemconcomp.2014.09.022>.
- 465 [8] J. He, X. Shi, Laboratory assessment of a self-healing system for early-age
466 durability benefits to cementitious composites, *Journal of Building Engineering*.
467 (2021) 102602. <https://doi.org/10.1016/j.jobe.2021.102602>.
- 468 [9] X. Wang, J. Liang, J. Ren, W. Wang, J. Liu, F. Xing, Performance of
469 microcapsule-based self-healing concrete under multiaxial compression with large
470 axial strain: Mechanical properties failure mode, and pore structure, *Construction
471 and Building Materials*. 350 (2022) 128866.
472 <https://doi.org/10.1016/j.conbuildmat.2022.128866>.
- 473 [10] H. Jonkers, E. Schlangen, Development of a bacteria-based self healing concrete,
474 *Tailor Made Concrete Structures*. (2008) 109–109. <https://doi.org/10/dgt799>.
- 475 [11] I. Justo-Reinoso, A. Heath, S. Gebhard, K. Paine, Aerobic non-ureolytic bacteria-
476 based self-healing cementitious composites: A comprehensive review, *Journal of
477 Building Engineering*. 42 (2021) 102834.
478 <https://doi.org/10.1016/j.jobe.2021.102834>.
- 479 [12] A. Raza, R. Arsalan Khushnood, Digital image processing for precise evaluation
480 of concrete crack repair using bio-inspired strategies, *Construction and Building
481 Materials*. 350 (2022) 128863. <https://doi.org/10.1016/j.conbuildmat.2022.128863>.
- 482 [13] A. Darquennes, K. Olivier, F. Benboudjema, R. Gagné, Self-healing at early-age, a
483 way to improve the chloride resistance of blast-furnace slag cementitious

- 484 materials, *Construction and Building Materials*. 113 (2016) 1017–1028.
 485 <http://dx.doi.org/10.1016/j.conbuildmat.2016.03.087>.
- 486 [14] I. Salama, B. Hilloulin, S. Medjigbodo, A. Loukili, Influence of supplementary
 487 cementitious materials on the autogenous healing of cracks in cementitious
 488 materials, in: *ACI Symposium Publication (ICCM 2017)*, 2017: p. 12.1-12.14.
- 489 [15] X. Hu, C. Shi, Z. Shi, B. Tong, D. Wang, Early age shrinkage and heat of
 490 hydration of cement-fly ash-slag ternary blends, *Construction and Building*
 491 *Materials*. 153 (2017) 857–865.
 492 <https://doi.org/10.1016/j.conbuildmat.2017.07.138>.
- 493 [16] P. Shen, L. Lu, Y. He, M. Rao, Z. Fu, F. Wang, S. Hu, Experimental investigation
 494 on the autogenous shrinkage of steam cured ultra-high performance concrete,
 495 *Construction and Building Materials*. 162 (2018) 512–522.
 496 <https://doi.org/10.1016/j.conbuildmat.2017.11.172>.
- 497 [17] A.R. Suleiman, A.J. Nelson, M.L. Nehdi, Visualization and quantification of crack
 498 self-healing in cement-based materials incorporating different minerals, *Cement*
 499 *and Concrete Composites*. 103 (2019) 49–58.
 500 <https://doi.org/10.1016/j.cemconcomp.2019.04.026>.
- 501 [18] M. Mohammadi, C. Youssef, M. Robira, B. Hilloulin, Self-Healing Potential and
 502 Phase Evolution Characterization of Ternary Cement Blends, *Materials*. 13 (2020)
 503 17. <https://doi.org/10.3390/ma13112543>.
- 504 [19] C. Youssef Namnoum, B. Hilloulin, F. Grondin, A. Loukili, Determination of the
 505 origin of the strength regain after self-healing of binary and ternary cementitious
 506 materials including slag and metakaolin, *Journal of Building Engineering*. 41
 507 (2021) 102739. <https://doi.org/10.1016/j.jobbe.2021.102739>.
- 508 [20] J. Sun, K.H. Kong, C.Q. Lye, S.T. Quek, Effect of ground granulated blast furnace
 509 slag on cement hydration and autogenous healing of concrete, *Construction and*
 510 *Building Materials*. 315 (2022) 125365.
 511 <https://doi.org/10.1016/j.conbuildmat.2021.125365>.
- 512 [21] K. Van Tittelboom, E. Gruyaert, H. Rahier, N. De Belie, Influence of mix
 513 composition on the extent of autogenous crack healing by continued hydration or
 514 calcium carbonate formation, *Construction and Building Materials*. 37 (2012) 349–
 515 359. <https://doi.org/10.1016/j.conbuildmat.2012.07.026>.
- 516 [22] K.R. Lauer, Autogenous healing of cement paste, in: *Journal Proceedings*, 1956:
 517 pp. 1083–1098.
- 518 [23] H.-W.W. Reinhardt, M. Jooss, Permeability and self-healing of cracked concrete
 519 as a function of temperature and crack width, *Cement and Concrete Research*. 33
 520 (2003) 981–985. <https://doi.org/10.1016/j.cemconres.2003.07.011>.
- 521 [24] K.R. Lauer, F.O. Slate, Autogenous healing of cement paste, *American Concrete*
 522 *Institute Journal*. 52 (1956) 1083–1097.
- 523 [25] B. Hilloulin, D. Hilloulin, F. Grondin, A. Loukili, N. De Belie, Mechanical regains
 524 due to self-healing in cementitious materials: Experimental measurements and
 525 micro-mechanical model, *Cement and Concrete Research*. 80 (2016) 21–32.
 526 <https://doi.org/10.1016/j.cemconres.2015.11.005>.
- 527 [26] N. Ter Heide, E. Schlangen, Self Healing of early age cracks in concrete, in:
 528 *Proceedings of the First International Conference on Self Healing Materials*,
 529 Noordwijk Aan Zee, The Netherlands, 18-20 April 2007, 2007.
- 530 [27] C. Joseph, D. Gardner, T. Jefferson, B. Isaacs, B. Lark, Self-healing cementitious
 531 materials: a review of recent work, *Proceedings of the Institution of Civil*
 532 *Engineers-Construction Materials*. 164 (2011) 29–41.
- 533 [28] W.P. Boshoff, G.P.A.G. van Zijl, Tensile creep of SHCC, (2007) 87–95.

- 534 [29] P. Jun, V. Mechtcherine, Behaviour of strain-hardening cement-based composites
535 (SHCC) under monotonic and cyclic tensile loading: Part 1 - Experimental
536 investigations, *Cement and Concrete Composites*. 32 (2010) 801–809.
537 <https://doi.org/10.1016/j.cemconcomp.2010.07.019>.
- 538 [30] V.C. Li, E.-H. Yang, *Self Healing in Concrete Materials*, (2007) 161–193.
539 https://doi.org/10.1007/978-1-4020-6250-6_8.
- 540 [31] S.Z. Qian, J. Zhou, E. Schlangen, Influence of curing condition and precracking
541 time on the self-healing behavior of Engineered Cementitious Composites, *Cement*
542 *and Concrete Composites*. (2010).
543 <https://doi.org/10.1016/j.cemconcomp.2010.07.015>.
- 544 [32] E. Özbay, M. Sahmaran, Effect of sustained flexural loading on self-healing of
545 engineered cementitious composites, *Journal of Advanced Concrete Technology*.
546 11 (2013) 167–179.
- 547 [33] G. Yildirim, Ö.K. Keskin, S.B.I. Keskin, M. Şahmaran, M. Lachemi, A review of
548 intrinsic self-healing capability of engineered cementitious composites: Recovery
549 of transport and mechanical properties, *Construction and Building Materials*. 101
550 (2015) 10–21. <https://doi.org/10.1016/j.conbuildmat.2015.10.018>.
- 551 [34] M. Irfan-ul-Hassan, B. Pichler, R. Reihnsner, Ch. Hellmich, Elastic and creep
552 properties of young cement paste, as determined from hourly repeated minute-long
553 quasi-static tests, *Cement and Concrete Research*. 82 (2016) 36–49.
554 <http://dx.doi.org/10.1016/j.cemconres.2015.11.007>.
- 555 [35] M. Smadi, O. Floyd, A.H. Nilson, Shrinkage and Creep of High-, Medium-, and
556 Low-Strength Concretes, Including Overloads, *ACI Materials Journal*. 84 (1987)
557 224–234.
- 558 [36] L. Ferrara, V. Krelani, A fracture testing based approach to assess the self healing
559 capacity of cementitious composites, in: *Proceedings of the 8th Conference on*
560 *Fracture Mechanics of Concrete and Concrete Structures*, 2013.
- 561 [37] L.-L. Kan, H.-S. Shi, A.R. Sakulich, V.C. et Li, Self-Healing Characterization of
562 Engineered Cementitious Composite Materials, *Journal of the American Concrete*
563 *Institute*. 107 (2010) 619–626.
- 564 [38] C. Youssef-Namnoum, B. Hilloulin, F. Grondin, A. Loukili, Modelling of
565 autogenous healing of cement paste followed by a sustained load, in: *10th*
566 *International Conference on Fracture Mechanics of Concrete and Concrete*
567 *Structures, FraMCoS-X, Bayonne (France), 2019*.
- 568 [39] N.T. Heide, *Crack healing in hydrating concrete*, Delft University of Technology,
569 2005.
- 570 [40] S. Bazant, Z.P., Prasannan, Solidification theory for concrete creep. I:
571 Formulation, *Journal of Engineering Mechanics*. 115 (1989) 1691–1703.
- 572 [41] B. Hilloulin, F. Grondin, M. Matallah, A. Loukili, *Cement and Concrete Research*
573 *Modelling of autogenous healing in ultra high performance concrete*, *Cement and*
574 *Concrete Research*. 61–62 (2014) 64–70.
575 <https://doi.org/10.1016/j.cemconres.2014.04.003>.
- 576 [42] P. Rossi, N. Godart, J.L. Robert, J.P. Gervais, D. et Bruhat, Investigation of the
577 basic creep of concrete by acoustic emission, *Materials and Structures*. 27 (1994)
578 510–514.
- 579 [43] N. Ter Heide, *Crack healing in hydrating concrete*, Delft University of
580 *Technology*, 2005.
- 581 [44] K.-S. Lauch, J.-P. Charron, C. Desmetre, Comprehensive evaluation of self-
582 healing of concrete with different admixtures under laboratory and long-term

583 outdoor expositions, Journal of Building Engineering. 54 (2022) 104661.
584 <https://doi.org/10.1016/j.jobe.2022.104661>.
585

Authors' version